
ORIGINAL ARTICLE

Journal Section

Recurrent Neural Network-based Model Predictive Control for Continuous Pharmaceutical Manufacturing

Wee Chin Wong¹ | Jiali Li¹ | Xiaonan Wang¹

¹Department of Chemical & Biomolecular Engineering, Faculty of Engineering, National University of Singapore, 4 Engineering Drive 4, Singapore 117585, Singapore

Correspondence

Xiaonan Wang, Department of Chemical & Biomolecular Engineering, Faculty of Engineering, National University of Singapore, 4 Engineering Drive 4, Singapore 117585, Singapore
Email: chewxia@nus.edu.sg

Funding information

The authors thank the MOE AcRF Grant in Singapore for financial support to the projects of Precision Healthcare Development, Manufacturing and Supply Chain Optimization (R-279-000-513-133) and Advanced Process Control and Machine Learning Methods for Enhanced Continuous Manufacturing of Pharmaceutical Products (R-279-000-541-114).

The pharmaceutical industry has witnessed exponential growth in transforming operations towards continuous manufacturing to effectively achieve increased profitability, reduced waste, and extended product range. Model Predictive Control (MPC) can be applied for enabling this vision, in providing superior regulation of critical quality attributes. For MPC, obtaining a workable model is of fundamental importance, especially in the presence of complex reaction kinetics and process dynamics. Whilst physics-based models are desirable, it is not always practical to obtain one effective and fit-for-purpose model. Instead, within industry, data-driven system-identification approaches have been found to be useful and widely deployed in MPC solutions. In this work, we demonstrated the applicability of Recurrent Neural Networks (RNNs) for MPC applications in continuous pharmaceutical manufacturing. We have shown that RNNs are especially well-suited for modeling dynamical systems due to their mathematical structure and satisfactory closed-loop control performance can be yielded for MPC in continuous pharmaceutical manufacturing.

KEYWORDS

Pharmaceuticals, Critical Quality Attributes, Recurrent Neural

Abbreviations: Active Pharmaceutical Ingredients, APIs; Model Predictive Control, MPC; Critical Quality Attributes, CQAs; Artificial Neural Networks, ANNs; Recurrent Neural Networks, RNNs

1 | INTRODUCTION

The pharmaceutical industry has a growing interest in addressing key challenges such as the reduction of waste, cost, footprint and lead-times by implementing the concept of continuous manufacturing [1, 2]. As a result, with the development in continuous manufacturing technologies and quality by design paradigm, there is a trend of increasing demand for more advanced model identification and process control strategies in the continuous pharmaceutical industry [1].

One emerging application area for continuous manufacturing is to extend the palette of permissible reaction conditions and enable reaction outcomes that are quite challenging when performed under batch conditions [3, 4, 5]. The production of Active Pharmaceutical Ingredients (APIs) is the core part of pharmaceutical manufacturing. As a result, many researchers have proposed or employed continuous manufacturing technologies in the production processes of complex APIs. The fact is that these reactions are generally both reversible and coupled with many side reactions, thereby leading to a highly non-linear nature of the reaction system. As a result, this imposes difficulty on model identification. In addition to that, the need to operate in tight and extreme conditions leads to needs in effective and sophisticated control strategies [6, 7, 8]. The control and model identification of these continuous API reactions are particularly challenging due to the complexity of the underlying phenomena and the associated ultimate impact on reaction yields, molecular structure, downstream processing and Critical Quality Attributes (CQAs) of final product.

Model-based advanced control technology is viewed to be vital for enabling continuous pharmaceutical manufacturing by improving control of CQAs. The system identification is an indispensable part of the control performance for the whole process. Many rigorous models have been proposed to describe different API reactions [6, 9, 10]. These physics-based models have a clear physical interpretation. However, they can suffer from a complicated structure and may incur excessive computational cost during on-line control. Moreover, in many nonlinear systems, it is extremely difficult and expensive to obtain an accurate model of the process from first principles [11]. In contrast, experimental, data-driven heuristic models are easier to get and with relatively simple mathematical descriptions [12]. Belonging to the data-driven methods, neural networks have been applied actively in chemical and biochemical processing industry, especially has been implementing in some complex non-linear processes where process understanding is limited [13, 14, 15, 16].

System identification in chemical engineering applications addresses temporal correlations and interactions amongst the various states and controlled variables of concern. It is generally recognized that Artificial Neural Networks (ANNs) have the universal capability of approximating any function. Compared to the typical feed-forward ANNs, the structure of RNNs is such that the latter are better suited for providing temporal predictions. RNNs are inherently structured to use the hidden variables as a memory to capture long-term dependencies and have self-feedback of neurons between and within the hidden layers. This feedback process means RNNs inherently possess a "deep" structure. RNNs have been widely used in sequence learning problems including scene labeling [17] and language processing [18], with good success. The authors of [19] provide an excellent overview of the applications of neural networks especially from a process systems engineering perspective. Thus, in our work, we study the implementation of a RNN for model identification, using a complex reaction in a single Continuous-Stirred Tank Reactor (CSTR) for pharmaceutical API production, as an exemplary reference.

Apart from the modeling of complex pharmaceutical reactions, how to design effective model-based control algorithms for continuous manufacturing is also a research focus in academic literature [20] and industry. In addition,

the United States Food and Drug Administration (FDA) has emphasized that, in order to take full advantage of the real-time release Process Analytical Technology (PAT) concept, continuous-flow reactions require on-line monitoring and feedback control [21]. Model-based control is an excellent framework to rigorously incorporate the information of new and existing PAT technologies, as they emerge or get developed.

The MPC method is widely used in industrial applications [22, 23, 24] and it has been applied in control of CQAs in continuous pharmaceutical manufacturing [10, 20]. In [10], the authors presented two plant-wide MPC designs for whole continuous pharmaceutical manufacturing pilot plant from chemical synthesis to tablets formation using the quadratic dynamic matrix control algorithm, an earlier form of MPC. It shows by monitoring CQAs in real time, Critical Process Parameters (CPPs) can be actively manipulated to enable more robust and flexible process operation via feedback control. The advantages of MPC compared to conventional Proportional-Integral-Derivative (PID) controllers are highlighted in [20] via comparison of the control strategies to a feeding blending unit used in continuous pharmaceutical manufacturing. In addition to the work done on MPC, RNNs had been proposed to be used in conjunction with MPC in previous studies. For example, [25] investigated the applicability of RNNs for control of non-linear dynamical systems. RNNs have been used for predictive control of CSTRs (for instance [26]) but these have been limited to relatively basic kinetics (e.g., single-step, irreversible kinetics $A \rightarrow B$). Furthermore, these MPC studies have rarely been applied to the most challenging and essential part in continuous pharmaceutical manufacturing of reactor control.

Our contribution is in demonstrating the applicability of a special class of neural networks, termed RNNs, for MPC applications relevant to relatively complex continuous pharmaceutical manufacturing reaction applications. This paper is organized as follows. Section 2 describes the plant model for system identification and case studies for control closed loop performance assessment. Section 3.1 explains the RNN-based system identification methodology. Section 3.2 contains the MPC formulation. Results and discussions are shown in Section 4.

2 | PLANT MODEL AND CONTROL CASE STUDIES

The following subsections describe (i) the true plant model for the purpose of simulation and system identification and (ii) case studies in the case of closed-loop control.

2.1 | Plant Simulator

We consider the following reaction system in the context of a single CSTR, as was previously studied by [27, 28]. Distinct from the literature, our work focuses on system identification using RNNs with a view towards closed-loop control via MPC. Referring to Eq.1, the feed species is A , the desired product is the intermediate R with species S being an undesired byproduct. The reactions are reversible and depending on the value of the manipulated variable(s).



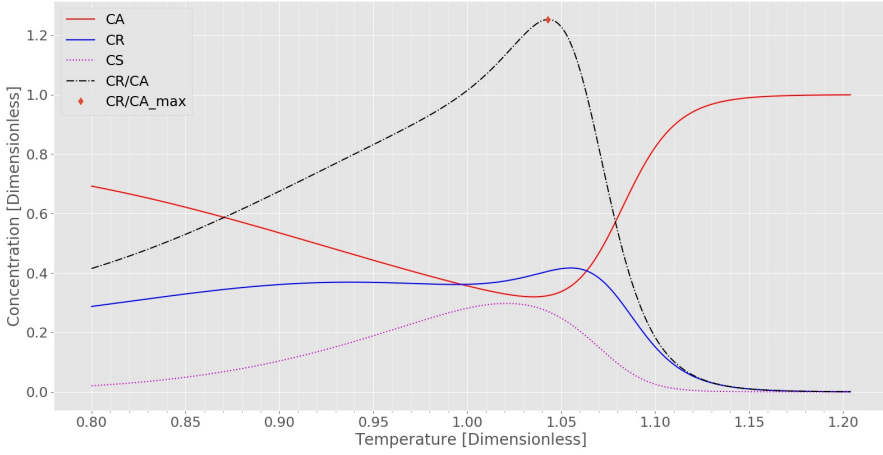


FIGURE 1 Steady-state conditions as a function of system temperature (with feed flow rate, $q = 0.8$)

The dynamic equations, based on normalized, dimensionless quantities are presented as such:

$$\begin{aligned}
 \frac{dC_A}{dt} &= q[C_{A0} - C_A] - k_1 C_A + k_4 C_R \\
 \frac{dC_R}{dt} &= q[1 - C_{A0} - C_R] + k_1 C_A + k_3[1 - C_A - C_R] - [k_2 + k_4]C_R \\
 k_j &= k_{0j} \exp \left\{ \left[-\frac{E}{RT_0} \right]_j \left[\frac{1}{T} - 1 \right] \right\}, j \in 1, 2, 3, 4
 \end{aligned} \tag{2}$$

Here, $C_j, j \in \{A, R, S\}$ refers to the concentration of the respective species within the reactor and form the state vector. The reactions are first-order, reversible with Arrhenius-type temperature dependencies. It is assumed that all concentrations are measured. The manipulated variables (MVs) are feed flow rate (q) and reactor temperature (T), whose values are also available. Here, it is assumed that the only species entering the CSTR are A and R such that their concentrations sum up to unity. As such, the concentration of species S is easily computed as a function of time. The values of the normalized feed concentrations, Arrhenius pre-exponentials and activation energies can be found in [28] and are reproduced in the Appendix for ease of reference.

As shown in Fig. 1, for a given flow rate, the concentration of the desired product, C_R reaches a maximum at a certain temperature, beyond which the reaction is driven all the way back to the left of Eq.1, yielding only feed reactant and no desired product, R . This problem possesses rich and relevant dynamics for continuous pharmaceutical manufacturing and is therefore worth detailed investigation. The control problem is challenging due to the existence of input multiplicities [27], [29]. In the sequel, we work in the discrete-time domain with time steps denoted by $k \in \mathbb{Z}^+$, as is common in digital control. Furthermore, we make the following definitions, $x \triangleq [C_A, C_R]'$, $u \triangleq [q, T]'$. The underlying

TABLE 1 Steady-state conditions (nominal flow rate, q , equals 0.8)

Scenarios	C_A (Feed)	C_R (Product)	q (Flow Rate)	T (Temperature)
(I) Startup	0.692	0.287	0.800	0.800
(II) Upset recovery	0.822	0.152	0.800	1.100
Set-point (maximum ratio of $C_R:C_A$)	0.324	0.406	0.800	1.043

plant may be described by a non-linear discrete-time difference equation of the form:

$$\begin{aligned}x_{k+1} &= \Phi(x_k, u_k) \\ y_k &= x_k\end{aligned}\quad (3)$$

where $k \in \{0, 1, 2, \dots\}$ is the discrete-time index, x_k the state variables, u_k , the manipulated variables. Full state feedback is assumed such that the measured output y_k equals the state vector at all time steps. $\Phi(\cdot)$ is the state-transition equation that is consistent with Eq.2 through numerical integration of the Ordinary Differential Equations (ODEs).

The problem of system identification as described in Section 3.1 is to find a representative approximation of Eq.3. In this paper, we assume that the p -step ahead prediction problem is of vital interest for the purpose of MPC. A sampling time, Δt of 0.1 (units of time) is used in this paper.

2.2 | Closed-Loop Control Case Studies

The approach taken in constructing a RNN for the purpose of MPC is to learn the RNN model with training data, and validate against previously unseen validation/ test data. However, given that the end goal is control, the final evaluation would be in terms of closed-loop performance for the two scenarios, relative to a benchmark/ reference Non-linear MPC (NMPC) approach that uses the true plant model (see ODEs in Eq.2) as the internal controller model for on-line control.

These scenarios are carefully selected and the corresponding conditions are described in Table 1. These exemplary scenarios are firstly, a (i) reactor system start-up case and secondly, (ii) an upset-recovery case where the controller needs to recover from an external upset. In the start-up scenario (case I), the system is assumed to be at an initial condition corresponding to a low temperature state that corresponds to relatively low product concentration. In the recovery scenario (case II), the system is assumed to be at an initial condition that corresponds to a region of relatively high temperature state and low yield.

The initial condition of the system corresponding to Case I is located on the left of peak C_R , as demarcated by an orange point in Fig. 2. The initial condition of the system corresponding to Case II is located to the right of the peak, as demarcated by the green point in Fig. 2. The set-point is judiciously chosen to be at a location where the ratio of product concentration to feed concentration is maximum and as is at a product concentration level that is only slightly lower than what is maximally achievable. The rationale is that this operating point maximizes yield whilst lowering downstream separations cost. Table 1 contains the initial steady-state values of the system as well as the target set-points.

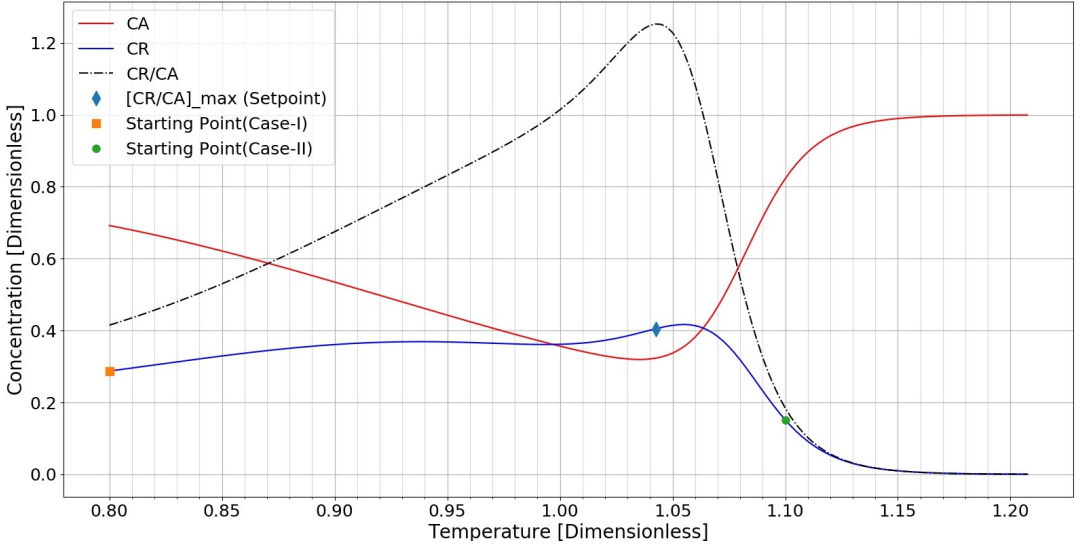


FIGURE 2 Starting conditions relative to set-point for case I (start-up) and case II (recovery)

3 | METHODOLOGIES

3.1 | Non-linear Time-Series System Identification via Recurrent Neural Networks

In our case, an MPC based on a single linear model would result in poor control performance due to the presence of input multiplicities corresponding to the change in gain. Thus, there is a need of a fit non-linear model for good closed-loop performance of the associated NMPC controller.

For clarity of exposition, consider a single RNN cell as follows (see Eq.4). At time step k , the hidden state variable of the RNN is the output of the cell and is denoted by h_k ; the input to the node is defined as u_{k-1} ¹.

$$h_k = \sigma(W_{h,h}h_{k-1} + W_{u,h}u_{k-1} + b_h) \quad (4)$$

where $\sigma(\cdot)$ is an activation function applied element-wise, $W_{u,h}$ is the input-to-hidden-state weight matrix; $W_{h,h}$ is the hidden-state-to-hidden-state weight matrix and b_h is a bias (offset) vector. The dimensionality of h and therefore that of $W_{u,h}$, $W_{h,h}$ and b_h depend on the number of nodes of the RNN cell. This single RNN cell can be unfolded across time-steps, as in Fig. 3 so that the temporal dependencies are clearly illustrated. Each cell may output directly to one or more measured observation vectors or output into one or more RNN layers above it (see Fig. 4). RNNs may be multi-layered where each subsequent layer captures more nuanced features than the prior layer.

At time step k , in order to make a p -step ahead prediction of the output variables, $\hat{y}_{k+p|k}$, a RNN, $\mathcal{N}(\cdot)$, is trained for the purpose of modeling the non-linear system dynamics. The corresponding regressors required to estimate this quantity is defined to be $\phi_k := [y_k, u_k, u_{k+1}, \dots, u_{k+p-1}]$. Note that the first element of the regressors is the output measurement at time-step k ; this is done as a way to provide some form of initialization for the hidden state at the first instance.

¹While the machine-learning literature does not account for a time-lag between input state and hidden state, we introduce a time-lag of 1 time-step so that the causal relationship is made explicit.

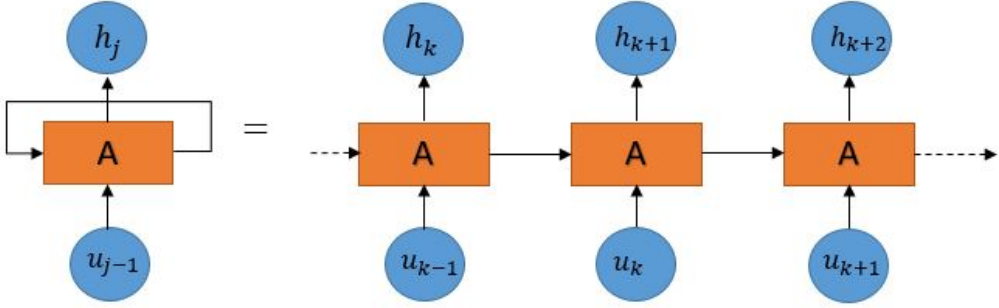


FIGURE 3 RNN - single cell (left) & unfolded across time (right)

The input sequences are introduced in a vertical, layered structure per Fig. 4. For MPC with a prediction horizon of p -steps, it is noted that the following equation is deployed as shorthand to describe the internal RNN-MPC model:

$$\hat{y}_{k+j|k} = \mathcal{N}(\phi_{k-p+j}), j \in \{1, 2, \dots, p\} \quad (5)$$

where the $\hat{(\cdot)}$ symbol makes explicit that an estimate is being computed.

The various weights are estimated by Back-Propagation Through Time (BPTT), which involves an application of the chain rule in the face of minimizing a certain loss function that is related to the prediction error of the model. In our study, the ‘Mean Absolute Error’ is adopted as the loss function. We employ the Adaptive Moment Estimation (ADAM) optimization algorithm [30], a popular stochastic gradient descent-like method with widely applicability, to learn the parameters and weights of the RNN.

The parameters associated with simple RNNs cells are known to be difficult to train due to the gradient-vanishing and gradient-exploding numerical problems. To resolve this, special RNN cell structures such as Long Short-Term Memory (LSTM) cells have been developed to address this issue. In the following cases, we used LSTMs to be the cell structure of interest. Details of the LSTM are left to the Appendix for interested readers.

3.2 | Control Problem Formulation

The fundamental strategy underpinning MPC is in the selection of a set of future control moves (spanning a control horizon of m steps) that minimizes a certain cost function based on the desired output trajectory over a prediction horizon (spanning p steps). MPC requires a reasonably accurate model, that captures the essential dynamics of the plant under control, so as to predict dynamic behavior multiple-steps ahead.

The following Receding Horizon Control (RHC) problem (Eq.6) is solved via a mathematical optimization program

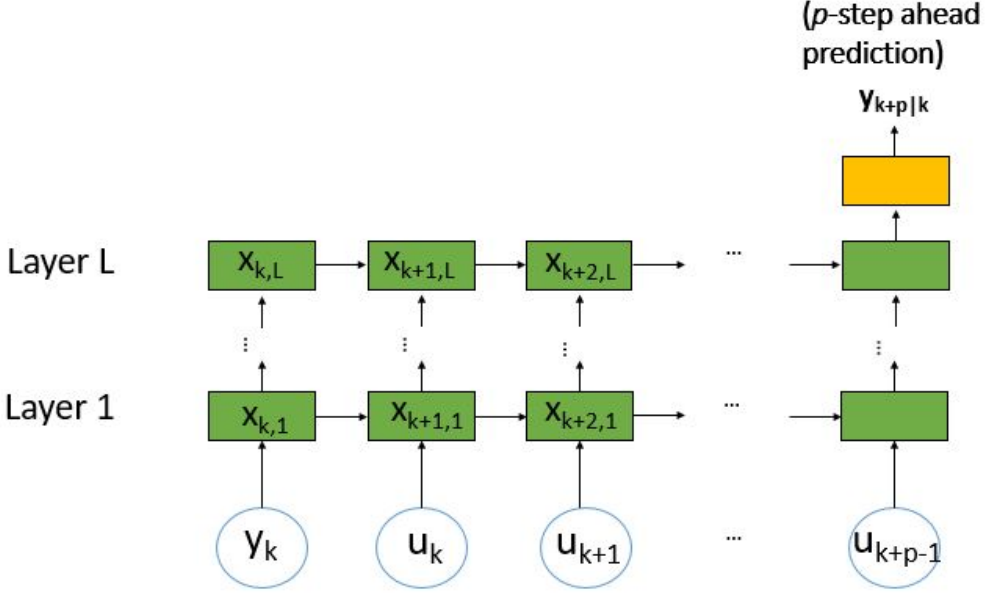


FIGURE 4 RNN structure for the p -step ahead prediction problem

at every time step k , whereupon new information in the form of y_k is made available.

$$\min_{\{\Delta u_k, \Delta u_{k+1}, \dots, \Delta u_{k+m-1}\}} \left\{ \sum_{j=1}^p (\hat{y}_{k+j|k} - y^*)' Q_y (\hat{y}_{k+j|k} - y^*) + \sum_{j=0}^{m-1} \Delta u'_{k+j} Q_u \Delta u_{k+j} \right\} \quad (6)$$

$$\hat{y}_{k+j|k} = N(\phi_{k-p+j}, j \in \{1, 2, \dots, p\}) \quad (7)$$

$$u_{k+i} \in [u_{\min}, u_{\max}], i \in \{0, 1, \dots, m-1\} \quad (8)$$

$$\Delta u_{k+i} \in [\Delta u_{\min}, \Delta u_{\max}], i \in \{0, 1, \dots, m-1\} \quad (9)$$

Here, vector y^* refers to the set-points of $[C_A^*, C_R^*]'$. $\Delta u_{k+j} \triangleq u_{k+j} - u_{k+j-1}$, refers to the discrete-time rate of change of the manipulated variables, where it is assumed that there is no change in actuator position beyond the control horizon. That is $\Delta u_{k+m} = \Delta u_{k+m+1}, \dots = 0, \forall k \in \mathbb{Z}^+$. $Q_y \in \mathbb{R}^{n_y \times n_y}$ and $Q_u \in \mathbb{R}^{n_u \times n_u}$ are square, symmetric, positive semi-definite weighting matrices that serve to penalize deviations from set-point and excessive actuator movement in a quadratic sense, as is typically used in MPC formulations. Constraints are imposed on both the absolute value of the manipulated variable as well as the rate of change, via respective upper and lower bounds, as shown in Eqs.(8)-(9).

The aforementioned optimization problem does not, in general possess special structures amenable to global optimality (e.g., convexity). This is a Non-Linear Programming (NLP) problem, which can be solved by modern, off-the-shelf solvers². At each time-step the optimal sequence (vector) of future actuator movements $\{\Delta u_k^*, \dots, \Delta u_{k+m-1}^*\}$ are computed whereupon the first element, Δu_k^* , is implemented and maintained until the next sampling instant, $k+1$. Thereafter, the optimization is repeated in a moving horizon fashion.

²For optimization during MPC, an off-the shelf optimizer based on Sequential Quadratic Programming (SQP), a popular method for solving non-linear constrained optimization problems, implemented in Python (`scipy.optimize.minimize`) was employed.

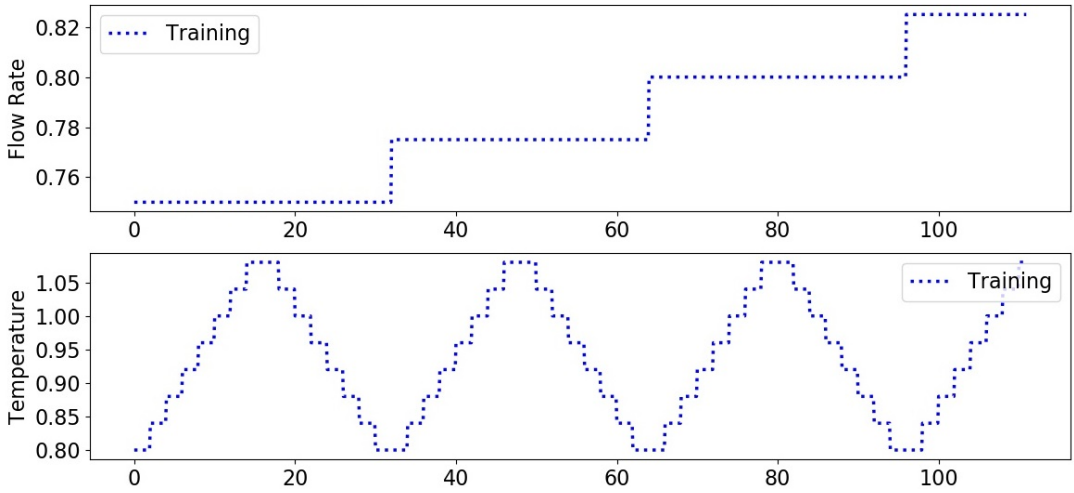


FIGURE 5 Training data for system identification (Manipulated Variable; sampling rate, $\Delta_t = 0.1$)

4 | RESULTS AND DISCUSSION

The procedure for investigating the RNN-MPC approach as a practical control strategy is according to the following steps: (1) Gathering process operating data with perturbation in all the manipulated variables to generate a rich-enough data set. (2) Training RNN models with various parameters using training sets and validating them with test data. Select the one with best performance that can capture most of the behavior of the plant. (3) Implementing the chosen RNN model into a properly designed MPC for the final purpose of control.

4.1 | System Identification Results

Using Eq.2 to simulate the true plant behavior, a profile of the manipulated variables per Fig. 5 was used to generate the necessary training data for the RNN model. Reactor temperature was stepped up (past the point of inflexion) and then back down for various choices of flow rates as can be seen in Fig. 5. The corresponding output profile for RNN can be found in Fig. 6. We varied the number of nodes between 250 to 2,000 and number of layers to be between 1 and 3. Table 2 summarizes the performance of the various RNN parameters over previously unseen test (validation) data. System identification performance over N data points is quantified by Root Mean Square Error (RMSE).

$$RMSE = \sqrt{\left(\frac{1}{N-p+1} \sum_{k=0}^{N-p} \{y_{k+p} - y_{k+p|k}\}^2 \right)} \quad (10)$$

Generally speaking, the prediction performance is found to improve with increasing number of nodes. This is because more expressive features are created when increasing number of nodes to better fit the nonlinear dynamic system behavior, thereby reducing prediction bias.

Furthermore, a deep, hierarchical model may be much more efficient in representing some functions than a shallow one [31]. We observed this when the number of layers were increased from 1 to 2. However, performance deteriorated when the number of layers were increased from 2 to 3.

TABLE 2 RMSE of RNN model over test data (1,000 training epochs)

No. Layers / No. Nodes	250	500	1000
1	0.0299	0.0268	0.0206
2	0.0238	0.0118	0.0083
3	0.0262	0.0119	0.0125

This is due to the fact that RNNs that are too deeply stacked may be difficult to learn, without extensive tuning potentially with heuristics and/or specially developed algorithms. This is potentially due to the aforementioned gradient vanishing numerical problems that arise during back-propagation. This issue is attributable to the complex structure of multi-layered RNN.

As can be seen in Table 2, using 1,000 nodes per RNN (LSTM) cell with 2 hidden RNN layers was found to yield the best prediction performance over previously unseen test data. Consequently, we opted to proceed in our system identification studies, and corresponding closed-loop control studies, by constraining the number of RNN layers to 2. For completeness, we also proceeded to learn an RNN model with 2 layers and 2,000 nodes. We noticed that over-fitting occurred, as reflected in Table 3.

TABLE 3 Performance of RNN model over test data for 2,000 nodes and 2 layers (1,000 training epochs). Results for 1,000 nodes and 2 layers are reproduced for ease of reference.

No. Layers	No. Nodes	RMSE (Test-Data)
2	1000	0.0083
2	2000	0.0177

The corresponding prediction performance for the best RNN on the training data (1,000 nodes and 2 layers) is shown in Fig. 6 and that on the test data can be seen in Fig. 7. For the case of the training data, it can be seen that there is very good fit. With highly dynamic input data, the resulting highly dynamic output information can be captured well. For the previous unseen test data, this well tuned RNN can show a good fit which captures all the general trend of the output information by given highly dynamic input data. Although the performance of the RNN for system identification of the test data is not perfect, it shows very promising result when implemented in MPC for closed-loop control purpose. The closed-loop results for 2 layers are shown in the following discussions³.

4.2 | Closed Loop RNN-MPC Performance

With reference to Fig. 2, for both cases, the objective is to have the system converge to a target set-point that corresponds to an operating point where the ratio of R concentration against that of A is at its maximum, thereby optimizing yield and potential downstream separation costs. It is noted that Linear MPC, based on a single linear model, will not be able to perform well [29], thereby necessitating the selection of a non-linear MPC solution.

For both scenarios, the following MPC controller parameters are used: $p = m = 1.0$ (time units), $Q_y = \text{diag}[2.4, 5.67]$, $Q_u = \text{diag}[25, 25]$. Total simulation time times, N , is set to 40.

³Code implementation is performed using the Python platform (ver 3.6.5) with Tensorflow (ver 1.7.0), equipped with a Keras (ver 2.1.5) interface for RNN learning. Numerical integration, where necessary, was performed using `scipy.integrate.ode` with a sample rate of 0.1 (time units).

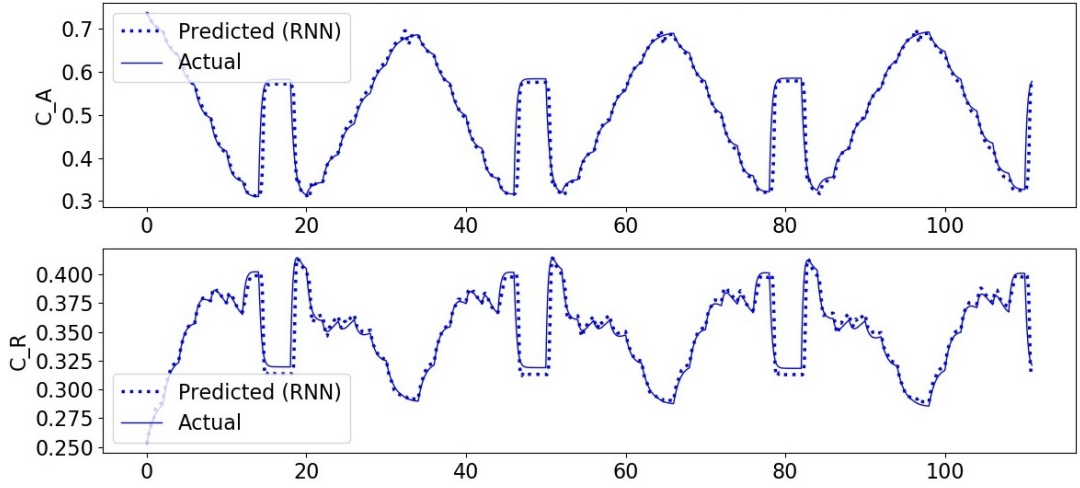


FIGURE 6 System identification - model p -step ahead prediction on training data [1000 nodes, 2 layers]

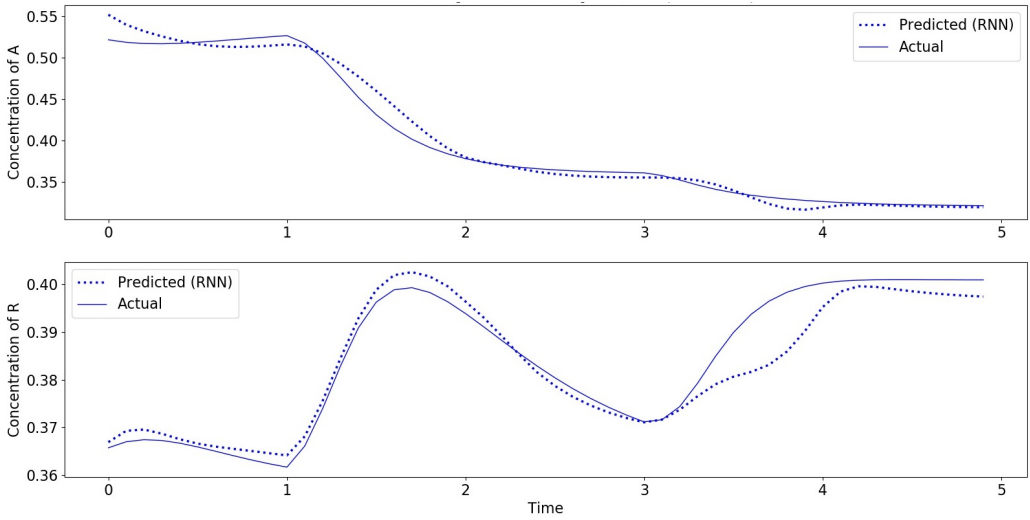


FIGURE 7 Model p -step ahead prediction on test data for system identification [1000 Nodes, 2 Layer]

The elements of Q_y are selected to reflect that tracking C_R is more important than tracking C_A . The Q_u penalty on excessive actuator movement Δu is higher than that on the state variables so as to avoid over-aggressive controller actions, which may lead to system instability.

For digital implementation, the sampling rate is $\Delta t = 0.1$ [dimensionless time units]. We assumed the flow rate and temperature to be constrained such that $q \in [0.75, 0.85]$, $T \in [0.5, 1.1]$. Also, the rate of change of the manipulated variables were constrained to be as such: $\Delta q \in [-0.1, 0.1]$ and $\Delta T \in [-0.1, 0.1]$, where the Δ operator represents time-differencing.

In the following studies, we perform closed-loop controller performance benchmarking. This is done against a NMPC controller where the controller's internal model is the same as the actual, full plant model (as in Eq. 3). The optimizer / solver deployed for both the RNN-MPC and benchmark NMPC methods remain the same as the one mentioned in the Section 3.2.

In comparing controller performance, the index used is naturally, the sum of the stage-wise MPC cost added over the total number of discrete-time steps, N , across the entire simulation horizon:

$$J = \sum_{k=1}^N \left\{ (y_k - y^*)' Q_y (y_k - y^*) + \Delta u_k' Q_u \Delta u_k \right\} \quad (11)$$

$$\mathcal{I} = \left\{ 1 - \frac{J_{[\text{RNN}]}}{J^*} \right\} * 100\% \quad (12)$$

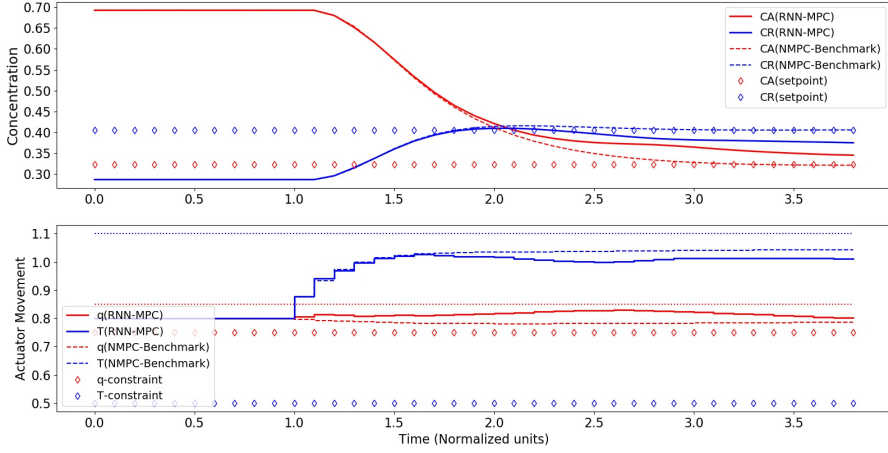
where Q_y , Q_u have already been defined in Eq.6 for the benchmark NMPC. The sequence of controller actions in Eq.11 are determined per the corresponding controllers. Specifically, $J_{[\text{RNN}]}$ refers to the corresponding total stage-wise cost for the RNN-MPC solution and J^* refers to that for the benchmark NMPC.

For both scenarios, the system is allowed to run for 1.0 time units (equivalent to the prediction horizon) before the controller is switched on. This is because the RNN-MPC is required to store in its memory a history of p number of manipulated input variables.

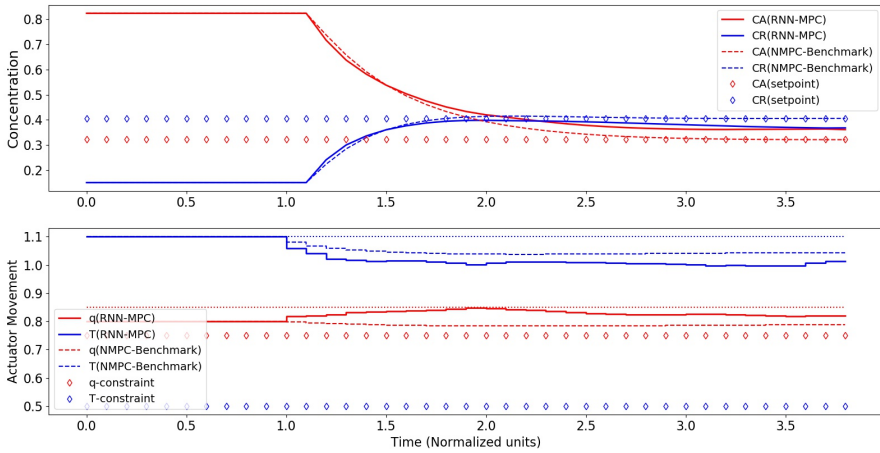
Figures 8-9 below and 10-11 in the Appendix show the closed-loop time-series for both scenarios as a function of different numbers of nodes. As can be seen from these plots, the RNN-MPC approach performs well for both complex control scenarios, in general. For example, all controllers exhibited stability, even in the under-fitted case of 250 nodes. This suggests a certain robustness associated with this combination. Table 4 summarizes a quantification of RNN-MPC performance by way of the closed loop performance index, averaged over both scenarios, for ease of comparison.

In the case of 250 nodes (see Fig. 8), it can be seen that a significant offset occurs at steady-state for both scenarios even though initial transient performance is somewhat similar to that of the benchmark NMPC solution. 1,000 nodes yielded the best closed-loop performance as evident in Fig. 9. This is consistent with the previous observations made during system identification. Steady-state tracking with no offset occurs for both scenarios. While the closed-loop trajectory of the RNN-MPC solution is close to that of the benchmark solution and has same total stage-wise cost as the benchmark NMPC solution. It is noted that in scenario 1, the transient performance is slightly more rapid than that of the benchmark. This is because the actuator movement, as informed by the SQP optimizer, is more aggressive (though still within the imposed constraints). In the case of 2,000 nodes (see Appendix Fig. 11), closed loop performance worsens as a result of over-fitting. We summarize the aforementioned discussion in Table 4, from which it is clear that 1,000 nodes yielded the best closed-loop performance.

In summary, these results illustrate that even if the open-loop system identification does not perfectly describe the actual true plant phenomenon, as long as the general trend and properties are captured, a RNN-MPC approach can lead to a good close-loop control performance. Under a practical situation, a perfect model is infeasible to get normally, our RNN-MPC approach can tackle with this situation well to get good control performance which shows a promising way

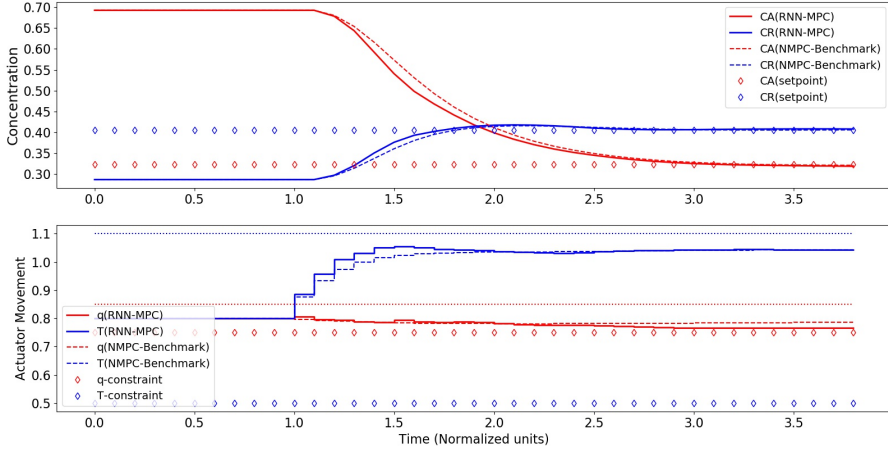


(a) 250 nodes; 2 RNN layers - startup

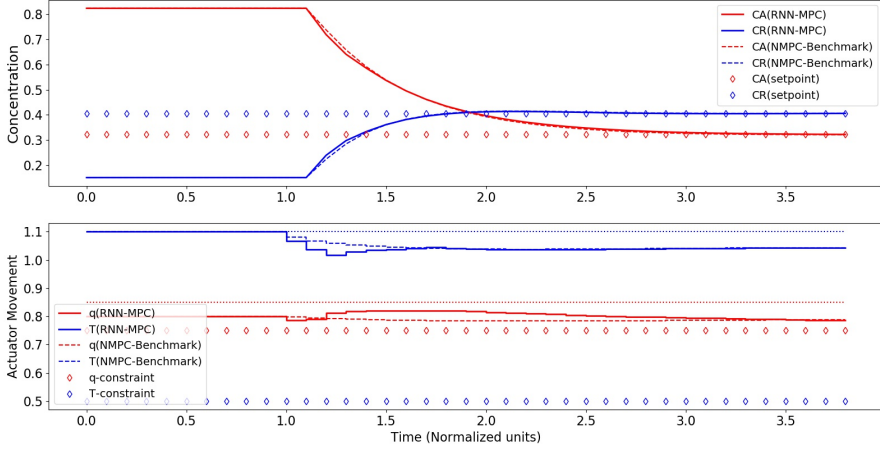


(b) 250 nodes; 2 RNN layers - recovery

FIGURE 8 Closed-loop performance with 250 nodes, 2 layers



(a) 1000 Nodes; 2 RNN layers - startup



(b) 1000 Nodes; 2 RNN layers - recovery

FIGURE 9 Closed-loop performance with 1000 nodes, 2 layers

TABLE 4 Performance of closed-loop RNN-MPC as a function of RNN nodes (2 layers)

No. Nodes	average performance index, \bar{I}_{avg}	Comments
250	93.7	Steady-state Offset
500	95.8	Steady-state Offset
1000	100.0	Desired Performance
2000	98.6	Steady-state Offset

to deal with real-world continuous pharmaceutical manufacturing challenges.

5 | CONCLUSION & FUTURE RESEARCH

We considered an exemplary problem for continuous pharmaceutical manufacturing by studying a single, multi-input multi-output CSTR example (per [28], [27]) which experiences input multiplicity due to reversible kinetics ($A \leftrightarrow R \leftrightarrow S$). This set-point is close to a point of inflexion where the system gain changes in sign with respect to reactor temperature.

We show how RNNs can be learned and present associated closed-loop performance results for two scenarios that require the RNN-based NMPC to move from either side of the inflexion point towards the desired set-point. As a result of input multiplicity, it is noted that a single linear controller will not work well for the problem of concern. While favorable results of the RNN-MPC controller are obtained when compared against a NMPC benchmark that uses the true plant model for control in terms of closed-loop performance.

Future research involves extending the methodology to multiple CSTRs and to reaction kinetics of increasing complexity and immediate relevance to the pharmaceutical industry.

ACKNOWLEDGEMENTS

We would like to acknowledge Associate Professor Saif A. Khan in the Department of Chemical and Biomolecular Engineering, National University of Singapore for his input related to reaction kinetics and multiple discussions. Also, our thanks to the Pharma Innovation Programme Singapore (PIPS), the source of motivation for this work.

CONFLICT OF INTEREST

We declare no conflict of interest.

REFERENCES

- [1] Lakerveld R, Benyahia B, Heider PL, Zhang H, Wolfe A, Testa CJ, et al. The application of an automated control strategy for an integrated continuous pharmaceutical pilot plant. *Organic Process Research and Development* 2015;19(9):1088–1100.
- [2] Schaber SD, Gerogiorgis DI, Ramachandran R, Evans JMB, Barton PI, Trout BL. Economic analysis of integrated continuous and batch pharmaceutical manufacturing: A case study. *Industrial & Engineering Chemistry Research* 2011 9;50(17):10083–10092.
- [3] Glasnov T. *Continuous-flow chemistry in the research laboratory*. Springer; 1st ed. 2016 edition (June 2, 2016); 2016.
- [4] Gutmann B, Cantillo D, Kappe CO. Continuous-flow technology - A tool for the safe manufacturing of active pharmaceutical ingredients. *Angewandte Chemie - International Edition* 2015;54(23):6688–6728.
- [5] Poehlauer P, Colberg J, Fisher E, Jansen M, Johnson MD, Koenig SG, et al. Pharmaceutical roundtable study demonstrates the value of continuous manufacturing in the design of greener processes. *Organic Process Research and Development* 2013;17(12):1472–1478.
- [6] Benyahia B, Lakerveld R, Barton PI. A plant-wide dynamic model of a continuous pharmaceutical process. *Industrial & Engineering Chemistry Research* 2012 11;51(47):15393–15412.
- [7] Susanne F, Martin B, Aubry M, Sedelmeier J, Lima F, Sevinc S, et al. Match-making reactors to chemistry: a continuous manufacturing-enabled sequence to a key benzoxazole pharmaceutical intermediate. *Organic Process Research & Development* 2017;21(11):1779–1793.

- [8] Mascia S, Heider PL, Zhang H, Lakerveld R, Benyahia B, Barton PI, et al. End-to-end continuous manufacturing of pharmaceuticals: Integrated synthesis, purification, and final dosage formation. *Angewandte Chemie International Edition* 2013 11;52(47):12359–12363.
- [9] Brueggemeier SB, Reiff EA, Lyngberg OK, Hobson LA, Tabora JE. Modeling-based approach towards quality by design for the ibipinabant API step modeling-based approach towards quality by design for the ibipinabant API step. *Organic Process Research and Development* 2012;16:567–576.
- [10] Mesbah A, Paulson JA, Lakerveld R, Braatz RD. Model predictive control of an integrated continuous pharmaceutical manufacturing pilot plant. *Organic Process Research & Development* 2017;21(6):844–854.
- [11] Hussain MA. Review of the applications of neural networks in chemical process control simulation and online implementation. *Artificial Intelligence in Engineering* 1999;13:55–68.
- [12] Cheng L, Liu W, Hou ZG, Yu J, Tan M. Neural-network-based nonlinear model predictive control for piezoelectric actuators. *IEEE Transactions on Industrial Electronics* 2015 Dec;62(12):7717–7727.
- [13] Xiong Z, Zhang J. A batch-to-batch iterative optimal control strategy based on recurrent neural network models. *Journal of Process Control* 2005;15:11–21.
- [14] Tian Y, Zhang J, Morris J. Modeling and optimal control of a batch polymerization reactor using a hybrid stacked recurrent neural network model. *Industrial & Engineering Chemistry Research* 2001;40(21):4525–4535.
- [15] Mujtaba IM, Hussain MA. Applications of neural networks and other learning technologies in process engineering. London, UK, UK: Imperial College Press; 2001.
- [16] Nagy ZK. Model based control of a yeast fermentation bioreactor using optimally designed artificial neural networks. *Chemical Engineering Journal* 2007;127(1-3):95–109.
- [17] Byeon W, Breuel TM, Raue F, Liwicki M. Scene labeling with LSTM recurrent neural networks. In: 2015 IEEE Conference on Computer Vision and Pattern Recognition (CVPR); 2015. p. 3547–3555.
- [18] Cho K, van Merriënboer B, Gülçehre Ç, Bougares F, Schwenk H, Bengio Y. Learning phrase representations using RNN encoder-decoder for statistical machine translation. *CoRR* 2014;1406.1078.
- [19] Lee JH, Shin J, Realf MJ. Machine learning: Overview of the recent progresses and implications for the process systems engineering field (in press). *Computers & Chemical Engineering* 2017 10.
- [20] Rehr J, Krusz J, Sacher S, Khinast J, Horn M. Optimized continuous pharmaceutical manufacturing via model-predictive control. *International Journal of Pharmaceutics* 2016;510(1):100–115.
- [21] Federsel H. Searching for scalable processes addressing the challenges in times of increasing complexity. current opinion in drug discovery & development. *U.S. Food and Drug Administration*; 2003.
- [22] Rawlings JB, Mayne DQ. Model predictive control: theory and design. Madison, WI, USA: Nob Hill; 2009.
- [23] Tatjewski P. Advanced control of industrial processes, structures and algorithms. London, U.K: Springer-Verlag; 2007.
- [24] Garcia CE, Morshedi AM. Quadratic programming solution of dynamic matrix control (QDMC). *Chemical Engineering Communications* 1986 7;46(1-3):73–87.
- [25] Pan Y, Wang J. Model predictive control of unknown nonlinear dynamical systems based on recurrent neural networks. *IEEE Transactions on Industrial Electronics* 2012;59(8):3089–3101.
- [26] Seyab RKA. Differential recurrent neural network based predictive control. *Computers and chemical engineering* 2008;32:1533–1545.

- [27] Koppel LB. Input multiplicities in nonlinear, multivariable control systems. *AIChE Journal* 1982;28(6):935–945.
- [28] Seki H, Ooyama S, Ogawa M. Nonlinear model predictive control using successive linearization - Application to chemical reactors. *Trans of the Society of Instrument and Control Engineers* 2004;E-3(1):66–72.
- [29] Bequette BW. Non-linear model predictive control : A personal retrospective. *The Canadian Journal of Chemical Engineering* 2007;85:408–415.
- [30] Kingma DP, Ba J. Adam: A Method for stochastic optimization. *Computing Research Repository* 2014;1412.6980.
- [31] Pascanu R, Gulcehre C, Cho K, Bengio Y. How to construct deep recurrent neural networks 2013;p. 1–13.

APPENDIX

| Kinetic Parameters for Plant Model

C_{A0} refers to the feed concentration of A and is assigned a value of 0.8. The vector of Arrhenius pre-exponentials k_0 are sequentially assigned values of [1.0, 0.7, 0.1, 0.006].

The normalized activation energies $-\frac{E}{RT_0}$ have values of [8.33, 10.0, 50.0, 83.3].

| Long Short-Term Memory Cells

In the conventional RNN structure, back-propagation through time results in the gradient signal being multiplied numerous times viz-a-viz the weights corresponding to the various connections (edges). Depending on the eigen-value of the associated weighting matrix, this leads to the either vanishing (eigen-value less than unity) or exploding (eigen-value greater than unity) gradients. This has the potential to severely impact the learning quality.

The machine-learning community has been using LSTM cells to replace the conventional RNN cell in order to mitigate this issue. These LSTM memory cell uses several gating functions that, in conjunction, serve to adjust / modulate the propagation of signals between cells (e.g., through ‘forgetting’, ‘input’, ‘output’ gates) to avoid said numerical issue.

The basic LSTM cell structure is as follows:

$$h_k = o_k * \tanh(C_k) \quad (13)$$

$$C_k = f_k * C_{k-1} + i_k * \tilde{C}_k \quad (14)$$

$$\tilde{C}_k = \tanh(W_C[h_{k-1}, u_{k-1}]' + b_c) \quad (15)$$

$$i_k = \sigma(W_i.[h_{k-1}, u_{k-1}]' + b_i) \quad (16)$$

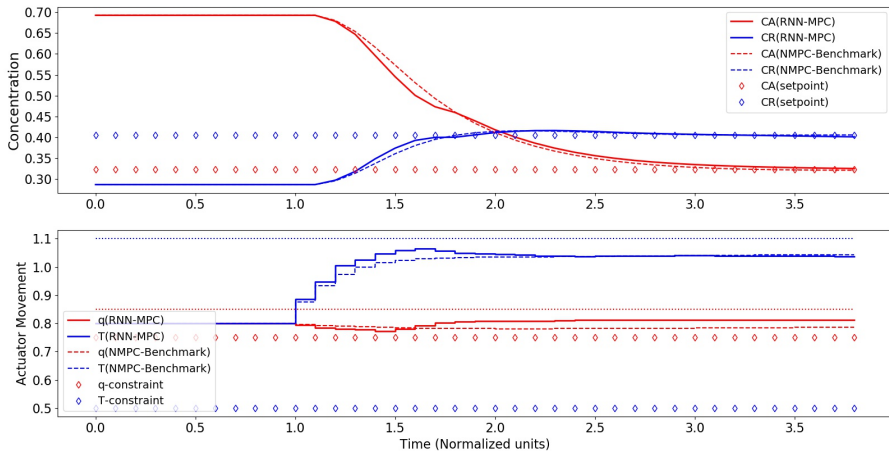
$$f_t = \sigma(W_f.[h_{k-1}, u_{k-1}]' + b_f) \quad (17)$$

$$o_t = \sigma(W_o.[h_{k-1}, u_{k-1}]' + b_o) \quad (18)$$

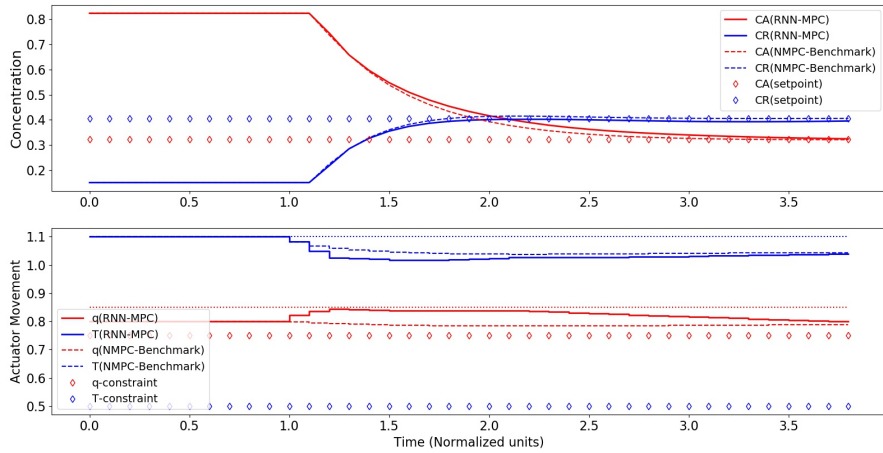
where k is the time index, h_k the hidden state variable, u_k the manipulated / input variable. $f_k \in [0, 1]$, $i_k \in [0, 1]$ and $o_k \in [0, 1]$ are termed the ‘forgetting’, ‘input’ and ‘output’ gates respectively. The input gate (Eq.16) controls the degree to which the state of the memory cell is affected by the candidate information (Eq.15); the output gate (Eq.18) controls how the state of the cell affects other neurons; the forget gate (Eq.17) modulates the cell’s self-recurrent connection, allowing the cell to (partially) remember the previous state, similar to traditional RNNs.

These work to combine old (C_{t-1}) and new candidate information (\tilde{C}_t), respectively, to be passed to subsequent LSTM cells. σ is an activation function that returns a value between 0 and 1. * refers to a point-wise multiplication.

Additional Figures - Closed Loop Performance

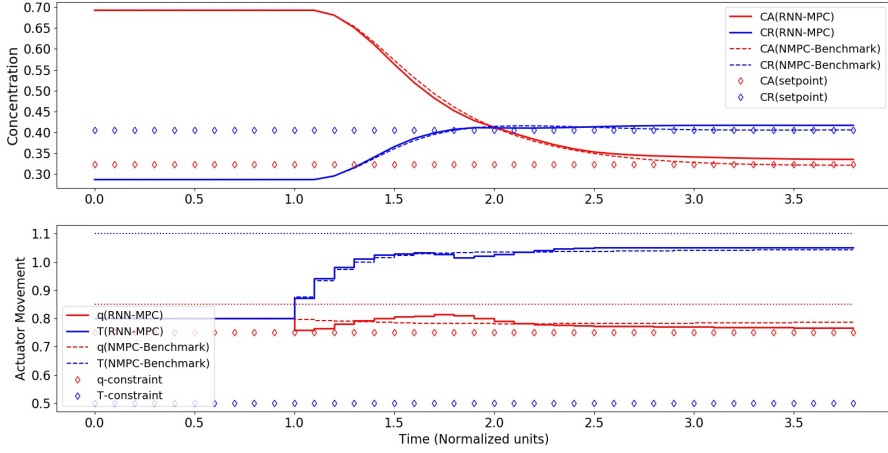


(a) 500 nodes; 2 RNN layer - startup

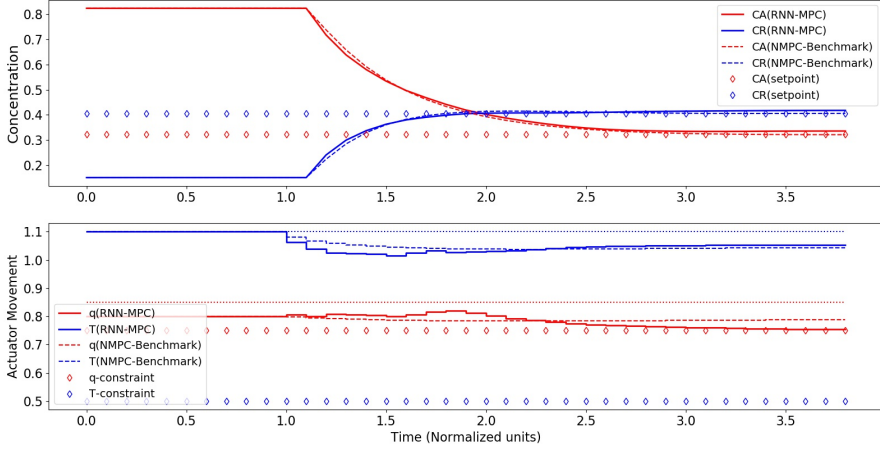


(b) 500 nodes; 2 RNN layer - recovery

FIGURE 10 Closed-loop performance with 500 nodes, 2 layers



(a) 2000 nodes; 2 RNN layers - startup



(b) 2000 nodes; 2 RNN layers - recovery

FIGURE 11 Closed-loop performance with 2000 nodes, 2 layers